Article:

Booth, AD and Pringle, JK (2016) Semblance analysis to assess GPR data from a five-year forensic study of simulated clandestine graves. Journal of Applied Geophysics, 125. pp. 37-44. ISSN 0926-9851

https://doi.org/10.1016/j.jappgeo.2015.11.016

Semblance analysis to assess GPR data from a five-year forensic study of simulated clandestine graves

Adam D. Booth[1*], Jamie K. Pringle[2]

1. a.booth@imperial.ac.uk; Department of Earth Science and Engineering, Imperial College London, South Kensington Campus, London, SW7 2AZ, UK

2. j.k.pringle@keele.ac.uk; School of Physical and Geographical Sciences, Keele University, Keele, Staffordshire ST5 5BG, UK

Abstract

Ground penetrating radar (GPR) surveys have proven useful for locating clandestine graves in a number of forensic searches. There has been extensive research into the geophysical monitoring of simulated clandestine graves in different burial scenarios and ground conditions. Whilst these studies have been used to suggest optimum dominant radar frequencies, the data themselves have not been quantitatively analysed. This study uses a common-offset configuration of semblance analysis both to characterise velocity trends from GPR diffraction hyperbolae and, since the magnitude of a semblance response is proportional to signal-to-noise ratio, to provide an objective measure of the strength of a GPR response. 2D GPR profiles were acquired over a simulated clandestine burial, with a wrapped-pig cadaver monitored at three-month intervals between 2008-2013 with

GPR antennas of three different centre-frequencies (110, 225 and 450 MHz). The GPR response to the cadaver was a strong diffraction hyperbola. Semblance analysis of profiles show little sensitivity to changes attributable to decomposition, and only a subtle influence of seasonality: velocity increases (0.01-0.02 m/ns) are observed in summer, associated with a decrease (5-10%) in peak semblance magnitude, S_M, and potentially in the reflectivity of the grave. The lowest-frequency antennas consistently give the highest signal-to-noise ratio although the grave was nonetheless detectable by all frequencies trialled. Whilst GPR analysis cannot currently provide a quantitative diagnostic proxy for time-since-burial, the consistency of responses suggests that graves may remain detectable beyond five years since creation. Furthermore, there is little seasonal influence on the detectability of a grave.

Graphical Abstract

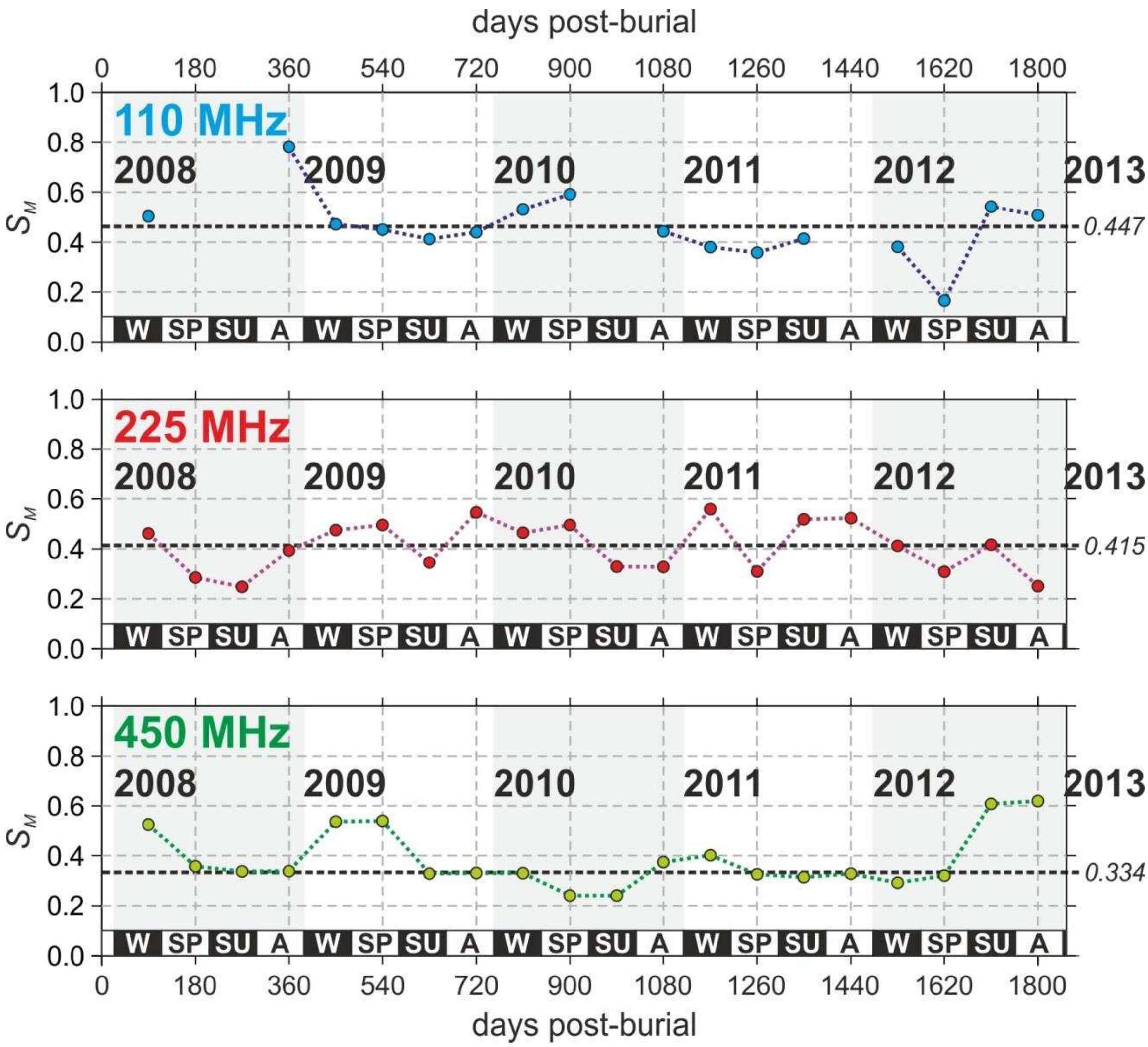

Highlights (max. 85 characters)

- Analysis of 2D GPR profiles acquired over simulated clandestine graves, with antenna frequencies of 110-900 MHz.
- Semblance analysis configured for analysis of diffraction hyperbolae in common offset data.
- Grave with wrapped-pig cadaver produces a consistent diffraction hyperbola, strongest in 110 MHz record.
- No long-term trend observed through the GPR record, suggesting wrapped burials may remain visible for longer than 5 years after burial.
- Subtle seasonality in GPR response, with semblance suggesting increased velocity and lower reflectivity during summer.

Keywords: forensic search; clandestine grave; GPR; semblance analysis

1. Introduction

There are numerous and varied methods employed by forensic search teams to detect the clandestine burial of murder victims (Pringle et al., 2012a; Parker et al., 2010). Current best practice suggests a phased approach, which moves from large-scale remote sensing methods (Kalacska et al., 2009) through to initial ground reconnaissance (Ruffell and McKinley, 2014) and control studies before full searches are initiated (Harrison and Donnelly, 2009; Larsen et al., 2011). These full searches have themselves involved a variety of methods including, for example, forensic geomorphology (Ruffell and McKinley, 2014), forensic botany (Aquila et al., 2014) and entomology (Amendt et al., 2007), scent-trained search dogs (Lasseter et al., 2003), physical probing (Ruffell, 2005a), thanatochemistry (Vass, 2012) and near-surface geophysics (see e.g. France et al., 1992; Powell, 2004; Nobes, 2000; Cheetham, 2005; Pringle and Jervis, 2009).

Near-surface geophysics appeals in forensic searches principally because of survey efficiency and non-invasiveness. Ground penetrating radar is arguably the most commonly used near-surface geophysical technique for clandestine grave detection (see e.g. Mellet, 1992; Calkin et al., 1995; Davenport, 2001; Ruffell, 2005b; Schultz, 2007; Billinger, 2009; Novo et al., 2011; Ruffell et al., 2014), and Nobes (2000) deploys the technique alongside electromagnetic prospection methods. Forensic burials differ strongly from historical and/or archaeological graves (e.g. Fiedler et al., 2009; Hansen et al., 2014). Archaeological examples can be difficult, though not impossible, to detect due to limited skeletal remains and processes of soil compaction (Vaughan, 1986); however, archaeological graves can be associated with monumental and/or ceremonial features, which are more readily detected. While the clandestine burial lacks any monumental features, organic remains are often present and the burial is typically shallow. As such, while archaeological survey methodologies may be replicated in forensic searches, the style and composition of the grave and its contents vary between the two settings.

Several recent GPR control studies use animal remains as a proxy for human remains in constructed graves, which are then repeatedly surveyed over extensive time periods (see e.g. France et al., 1992; Buck, 2003; Schultz et al., 2006; Schultz, 2007; Pringle et al., 2008; Schultz, 2008; Schultz and Martin, 2011; Pringle et al., 2012b; Schultz and Martin, 2012). These studies aim to determine optimal antenna centre-frequencies for numerous variables, including different time periods post-burial, varied burial styles, different soil types and local depositional environments. However, the assessment of GPR results has largely been visual, qualitative and/or subjective (Pringle et al., 2012b). This contrasts with a recent example of resistivity analysis, in which an objective and quantitative approach to characterising electrical responses was developed (Jervis and Pringle, 2014).

In this study, we develop a semblance-based method to objectify the assessment of a time-lapse archive of GPR observations from a simulated clandestine burial site. Semblance analysis, familiar for applications to data in the common midpoint (CMP) domain, is adapted for application to profiles of common offset GPR data. We demonstrate using synthetic data that the peak magnitude of the semblance response can be used as an indicator of signal-to-noise ratio, which in turn is suggestive of the underlying reflectivity of the target. We then consider the implications of semblance responses for the interpretation of real data. We observe a small seasonality in the peak semblance magnitude, likely related to soil moisture fluctuations but having only a minor impact on target detectability. A forensic search team could therefore anticipate that the GPR response to a burial will be constant throughout the year, and the results of the survey will be largely unaffected by local variations in soil condition.

2. Methods

Here, we describe the existing archive of pre-recorded GPR data, and describe our use of semblance analysis as a quantitative assessment tool.

2.1. Study background

This study focuses on the GPR archive of time-lapse geophysical observations acquired at a test site, where buried pig cadavers were used as a proxy for clandestine graves (Pringle et al. 2012b). The site is former garden land in the campus of Keele University (Staffordshire, UK) and is deemed typical of a semi-rural environment in the UK. The soil at the site is predominantly sandy loam, above the local water table, with fragments of shallow sandstone bedrock present at depths below ground level exceeding 0.5 m. Three graves were dug at an interval of approximately 4 m, to a depth of 0.5 m (representing a clandestine grave construction halted when encountering hard rock fragments). A pig cadaver weighing approximately 80 kg was placed in two graves before backfilling; the third grave was left empty and backfilled as a control. One pig cadaver was left naked (termed the '*naked-pig grave*') and the second was wrapped in a porous tarpaulin (termed the '*wrapped-pig grave*') (Jervis et al., 2009), to simulate two common conditions of murder victims. The study site remained dedicated as such throughout the study period and was subject to no change for its duration excepting natural processes. Extended discussion of the construction of the test site, and of the full suite of geophysical archives, is given in Jervis et al. (2009), Pringle et al. (2012b) and Jervis and Pringle (2014). In this analysis, we consider only the GPR profiles acquired over the *wrapped-pig* grave.

2.3 GPR survey data collection and basic processing

GPR profiles were repeatedly collected over the five year monitoring period, at intervals of approximately 3 months. Sensors&Software *PulseEKKO1000*™ equipment was used to collect 2D common offset (CO) profiles, using antenna sets of 110 MHz, 225 MHz, and 450 MHz centre-frequency (acquisition parameters listed in **Table 1**). Throughout, vertical stacking was set to 32. Data were processed in Sandmeier ReflexW© software, using sequential 'dewow' and Ormsby bandpass filters, static corrections to align time-zero within each trace, and a gain function based on the energy decay curve within each trace (**Table 2**). No form of migration is applied since this would collapse the diffraction hyperbolae which are the key focus of our analysis. Additionally, there is no topographic variation across the site hence static corrections are constant for each profile.

Representative time-lapse profiles acquired over the wrapped-pig grave are shown in **Figure 1**, the full suite of which is later supplied to semblance analysis for additional characterisation. The response to the wrapped-pig burial was a diffraction hyperbola, typically prominent throughout the survey period for all antenna frequencies acquired.

Table 1. Acquisition and relevant processing parameters for GPR profiles used in this study.

Centre-frequency (MHz)	Spatial sampling interval (m)	Temporal sampling interval (ns)	Antenna separation (m)
110	0.20	0.8	1.00
225	0.10	0.4	0.50
450	0.05	0.2	0.25
900	0.025	0.1	0.17

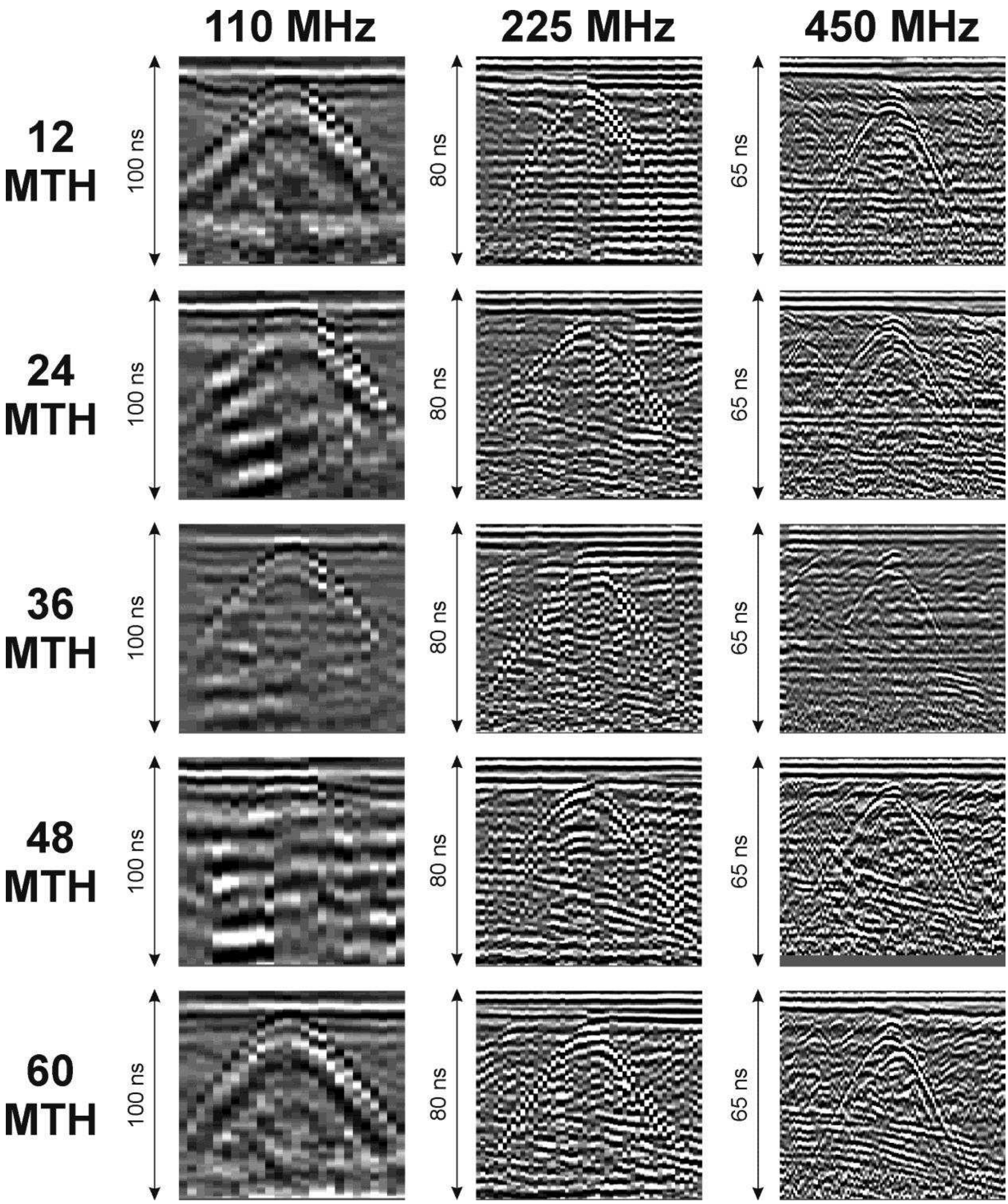

Fig. 1. Representative GPR 2D profiles, from 110, 225 and 450 MHz records over the wrapped-pig grave, acquired 12, 24, 36, 48 and 60 months after the creation of the graves. All profiles were 5 m wide. After Pringle et al. (2012b).

2.4 Semblance as a measure of data quality

Semblance is commonly applied in seismic and GPR velocity analysis routines (see, e.g., Yilmaz, 2001; Porsani *et al.*, 2006; Fomel and Landa, 2014), which seek to derive a subsurface velocity distribution from travel-time relationships in a dataset. Typically, semblance analysis is applied to reflection hyperbola in the common midpoint (CMP) domain, where the travel-time, $t(x)$, of energy reflected from the horizontal base of homogeneous, isotropic, overburden is approximated by the 'normal moveout' (NMO) equation:

$$t(x)^2 = t_0^2 + (x^2 / V_{ST}^2), \qquad \text{(Eq. 1)}$$

where x is the source-receiver offset, t_0 is the travel-time to that base at $x = 0$, and V_{ST} is termed 'stacking velocity', a near-offset approximation to root-mean-square velocity V_{RMS}. For the case of a single overburden layer, V_{RMS} is equivalent to interval velocity, V_{INT}, the propagation velocity within any one interval of the subsurface. The semblance statistic then provides a measure of the coherency of energy along trial trajectories defined by the substitution of trial pairs of V_{ST} and t_0 into Equation (1).

However, the data considered in this study were profiles of common offset (CO) data and the responses to be analysed in semblance analysis were diffraction, rather than reflection, hyperbolae. As such, the NMO equation was reconfigured for diffraction trajectories in the CO profile, such that travel-time, $t(x)$, was approximated as:

$$t(x)^2 = t(x_0)^2 + (4(x-x_0)^2/v_{ST}^2), \qquad \text{(Eq. 2)}$$

with x redefined as the position along a profile, x_0 as the surface position vertically above the diffracting target and $t(x_0)$ as the travel-time to the target when antennas are positioned at x_0 (see Ristic *et al.*, 2009). By substituting trial x_0, $t(x_0)$ and V_{ST} values into Equation (2), semblance is therefore measured along trajectories corresponding to diffraction hyperbolae in the GPR profile.

In addition to the objective definition of a subsurface velocity distribution from diffraction hyperbolae (as opposed to subjective curve-fitting), the semblance statistic could also provide an objective measure of data quality in terms of velocity resolution and signal-to-noise ratio (SNR). Assuming that the only changes within a time-lapse dataset are related to subsurface processes, and not environmental ones (e.g., ambient noise level), the changing semblance response could provide a proxy for the evolving reflectivity of the target and/or its detectability against background noise levels.

The relationship between signal-to-noise ratio and semblance-derived parameters was explored for synthetic GPR data (**Fig. 2a**), simulated using GprMax (see Giannopoulos, 2005). Specifically, synthetic data were used to investigate how variations in SNR are manifested in the peak magnitude and the velocity resolution expressed by a semblance response. The simulation represented the GPR response over a point diffractor, located at a depth of 0.7 m within a homogeneous layer of constant interval velocity of 0.12 m/ns; the GPR pulse was approximated by a 500 MHz Ricker wavelet, transmitted from a monostatic antenna with a spatial sampling interval of 0.01 m. Normally-distributed random noise amplitudes were scaled and added to the synthetic data, to give SNR of +10 dB. The semblance response (**Fig. 2b**), computed in Mathworks *Matlab*® for ranges of V_{ST} and $t(x_0)$ substituted into Equation (2), showed a characteristic arrangement of peaks which correspond to the slower stacking velocities expressed by successive wavelet half-cycles, given their increasing delay from first-break (see Booth *et al.*, 2010a for background). Semblance trajectories were defined for an aperture of 240 traces, i.e., for x = 1.2 m either side of the target diffraction (blue box in **Fig. 2c**), located vertically beneath x_0 = 2.5 m. The source pulse is dominated by the second wavelet half-cycle (**Fig. 2c**), hence the peak semblance magnitude, S_M (a dimensionless quantity), was measured for the second semblance peak; here, S_M = 0.703. The half-width of the same semblance peak spanned a range of stacking velocities from ~ 0.117 m/ns to 0.127 m/ns, hence v_{ST} resolution is the velocity enclosed by this range, ≈ 0.01 m/ns.

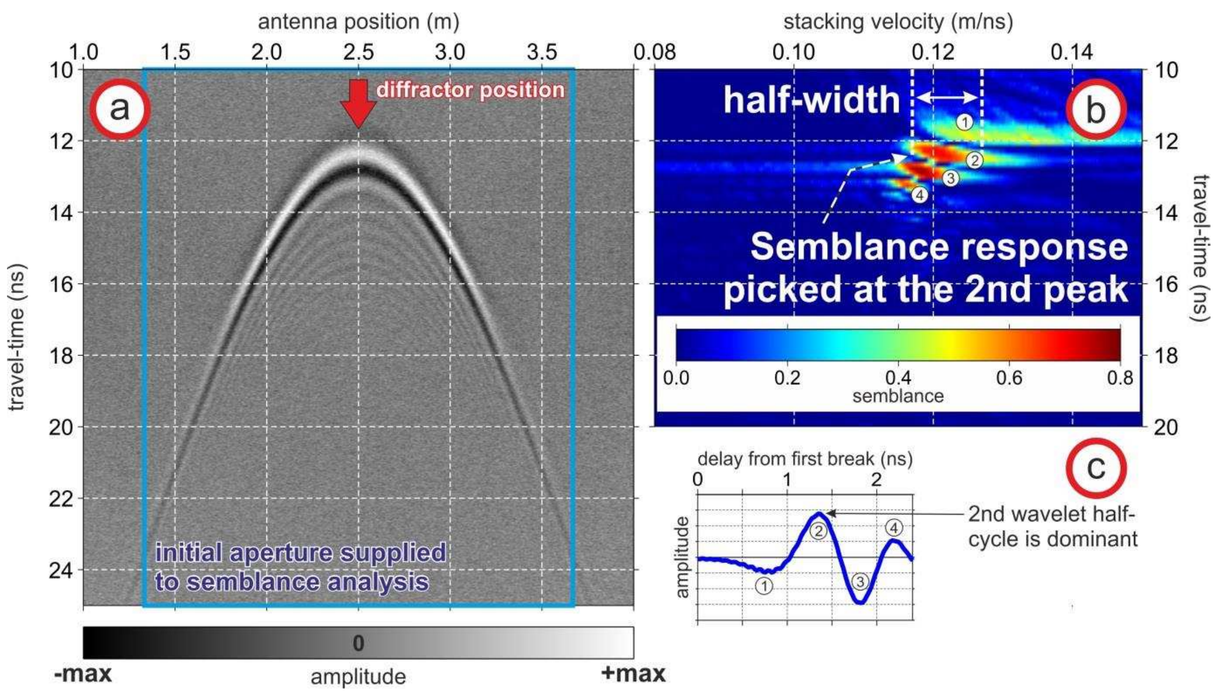

Fig. 2. Synthetic 500 MHz GPR diffraction hyperbola (a), showing the response to a point diffractor. The semblance response (b) is calculated within a 2.4 m-wide

aperture. The second semblance peak is picked, since this corresponds to the largest-magnitude of the four wavelet half-cycles labelled in (c).

Since semblance is a measure of wavelet coherency, an increase in the underlying noise level (i.e., a reduction in SNR) should reduce S_M. In **Figure 3a**, S_M is measured for the synthetic data as SNR is increased from -10 dB to +20 dB, and reduces sharply for SNR < +2.5 dB. For the time-lapse applications of this study, assuming that noise is stationary, S_M would be expected to vary as (e.g.) the reflectivity of the target changes, or with changes to the attenuation characteristics (typically associated with changing water saturation) of the overburden. Given the link to water saturation, the latter process may also be associated with a reduction in v_{ST}.

The resolution of stacking velocity v_{ST} in a semblance panel is a function of the travel-time moveout (the difference between $t(x)$ and $t(x_0)$) displayed by a diffraction hyperbola; the greater the moveout that is expressed, the better the resolution of v_{ST} will be (Booth *et al.*, 2011). If a wavelet undergoes greater attenuation, it follows that it will be visible in an increasingly narrow aperture around the diffraction hyperbola, and therefore display less travel-time moveout. We simulated this effect in **Figure 3b** by reducing the semblance aperture across which the synthetic data were analysed, from 2.4 to 0.4 m (corresponding to travel-time moveout reducing to 0.5 ns). The curves in this plot span the half-width of the resulting semblance peaks (as shown in **Fig. 2b**), therefore a narrower span implies superior resolution. Note that this 'funnel-shaped' plot was observed by Booth *et al.* (2011) for semblance analysis of CMP gathers, suggesting that the behaviour of the semblance statistic is independent of the domain in which it is applied. For a fixed analysis aperture, the resolution of velocity can also be used as a proxy SNR, since a higher-amplitude wavelet will be perceptible across a longer moveout range.

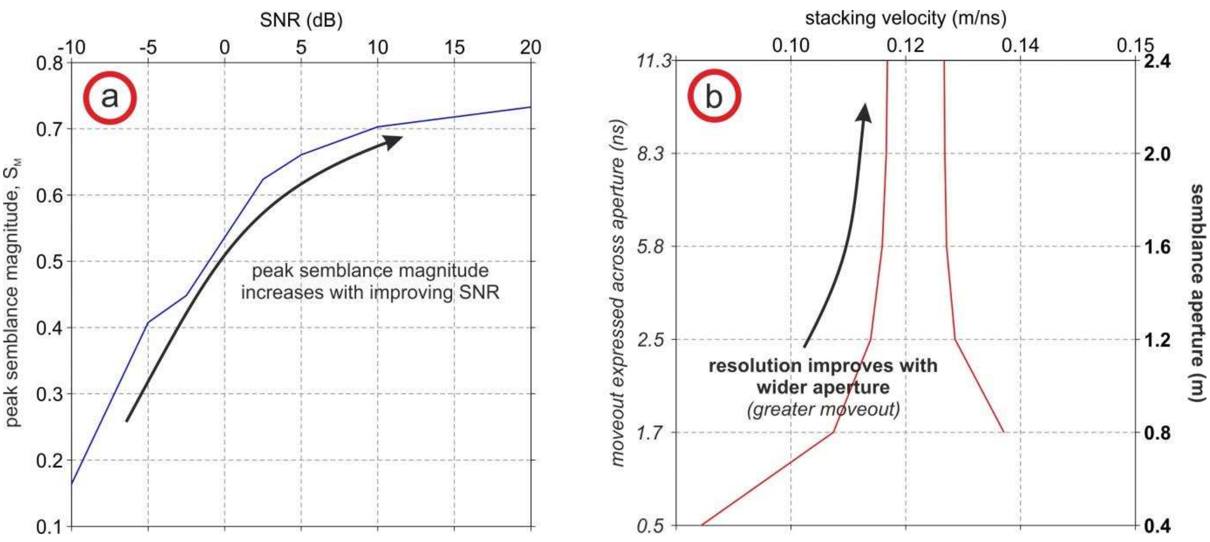

Fig. 3. Characteristics of semblance responses for modified synthetic data. a) Peak semblance magnitude, S_M, is increased for higher SNR within the synthetic data. b) The half-width of semblance peaks spans a narrower range of stacking velocity (i.e., improved resolution) for hyperbolae perceived across a wider aperture, corresponding to a longer travel-time moveout.

3. Data Analysis

Characteristics of the semblance response were used to quantify the assessment of GPR data quality. For all data analysed, we recorded:

1) the peak magnitude of the semblance response, S_M, to the diffraction hyperbola within each input profile;
2) the stacking velocity (v_{ST}) at which S_M is expressed;

3) the half-width of the peak semblance response, to quantify the resolution of v_{ST}, and;
4) the travel-time, $t(x_0)$, at which S_M is expressed.

While quantifying the assessment of GPR data quality, any systematic variation in these quantities could also be diagnostic of some decompositional process acting on the burials, or a change in the local overburden.

All GPR profiles were exported from ReflexW© processing software into Mathworks Matlab® for semblance analysis, and continuous time series of semblance characteristics could be derived for the five-year study period. All semblance analyses considered a range of trial stacking velocities from 0.05-0.12 m/ns, in increments of 0.0001 m/ns. The reference position, x_0, was taken in all cases to be 2.4 m (the position of the trace in which the apex of the diffraction hyperbola was perceived), and $t(x_0)$ spanned a range from 0-30 ns in increments equal to the temporal sampling interval of the input data (see **Table 1**). The semblance analysis window also spanned an interval equivalent to one temporal sample, to give the highest-resolution semblance response (see Booth *et al.*, 2011 for background). The analysis aperture was fixed at 4 m in all cases, consistent with the widest range of traces over which the diffraction hyperbola could be perceived.

4. Results

Figure 4 shows diffraction hyperbolae in GPR 2D profiles, and their corresponding semblance responses. This illustrative example, shown here for profiles acquired over the graves one year after their creation (the ‘12 MTH’ set of profiles in **Fig. 1**), was repeated for all profiles in the study. The hyperbolic curves which overlie the profiles were defined by substituting the V_{ST} and $t(x_0)$ pair expressed at the peak semblance response (as annotated in **Fig. 4**) into Equation (2). The 110 MHz response showed the highest peak semblance (> double that of the other diffractions) but, consistent with its lower frequency (Booth *et al.*, 2011), the poorest velocity resolution.

Although the 2D profiles were acquired over the same target, each hyperbola expressed a different stacking velocity and travel-time. This effect was partly attributable to effects of target geometry (i.e., the size of the target scattered different components of each frequency-limited wavelet), but also to the incorrect assumption in Equation (2) that there is zero offset between antennas (i.e., a monostatic GPR system). No correction was made for this since it would require a priori knowledge of the RMS velocity, but the necessary travel-time corrections could be included into the semblance analysis if required. Nonetheless, the semblance parameters we obtained should not be interpreted in terms of absolute subsurface properties (e.g., dielectric permittivity, or target radius; see Shihab and Al-Nuaimy, 2005; Ristic *et al.,* 2009 for background); instead, they were simply the quantities that the hyperbolae express. However, since the geometry of the acquisition never changed through the survey period, relative differences between successive semblance responses could be related to a change either in subsurface properties or ambient conditions.

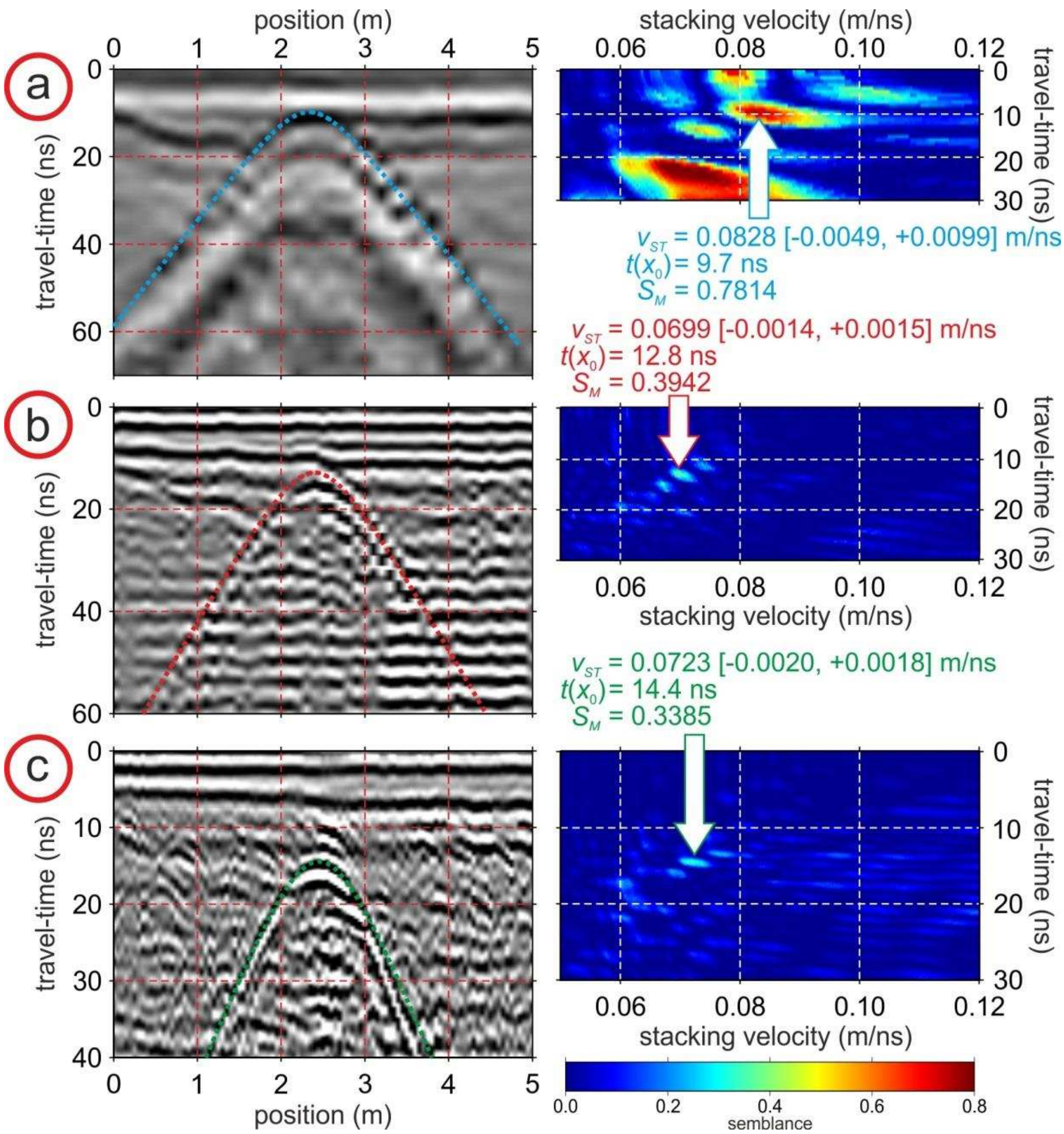

Fig. 4. Representative GPR 2D profiles acquired 12 months after burial, with corresponding calculated semblance analyses for (a) 110 MHz, (b) 225 MHz and (c) 450 MHz data. Arrows and corresponding annotations in semblance panels (right) indicate the respective peak semblance response.

The time series for v_{ST}, v_{ST} resolution and $t(x_0)$ are shown in **Figure 5**. Resolution was represented by the vertical v_{ST} error bar, and the colour of the symbol corresponds to $t(x_0)$. The time series of semblance magnitude is shown in **Figure 6**. Abbreviations W, SP, SU and A correspond respectively to seasons of the year (defined here as the complete months of January-March for winter, April-June for spring, July-September for summer, and November-December for autumn).

No long-term trend was perceived through the observations for the wrapped-pig grave, for any semblance parameter or indeed antenna frequency; however, there was limited seasonality indicated within the V_{ST} and S_M series. Stacking velocities tended to increase during the spring and summer months (an increase of ~0.01-0.02 m/ns compared to winter and autumn). This observation was consistent with soil moisture budget calculations of Jervis and Pringle (2014), who showed that the site was significantly drier during summer. These trends were supported by crossplots in which V_{ST} data are separated according to the season acquired (**Fig. 7**).

In contrast to V_{ST}, semblance magnitudes exhibited reductions (~5-10%) in spring and summer compared to their values in autumn and winter, potentially suggesting that the reflectivity of the wrapped-pig burial is weakest when the soil was driest (i.e., a stronger dielectric contrast exists between the grave and a moist soil). This effect was most apparent in the 450 MHz record; in the crossplot in Figure 7c, V_{ST} and S_M are anti-correlated, but the equivalent relationship is weaker for the 110 and (especially) 225 MHz records.

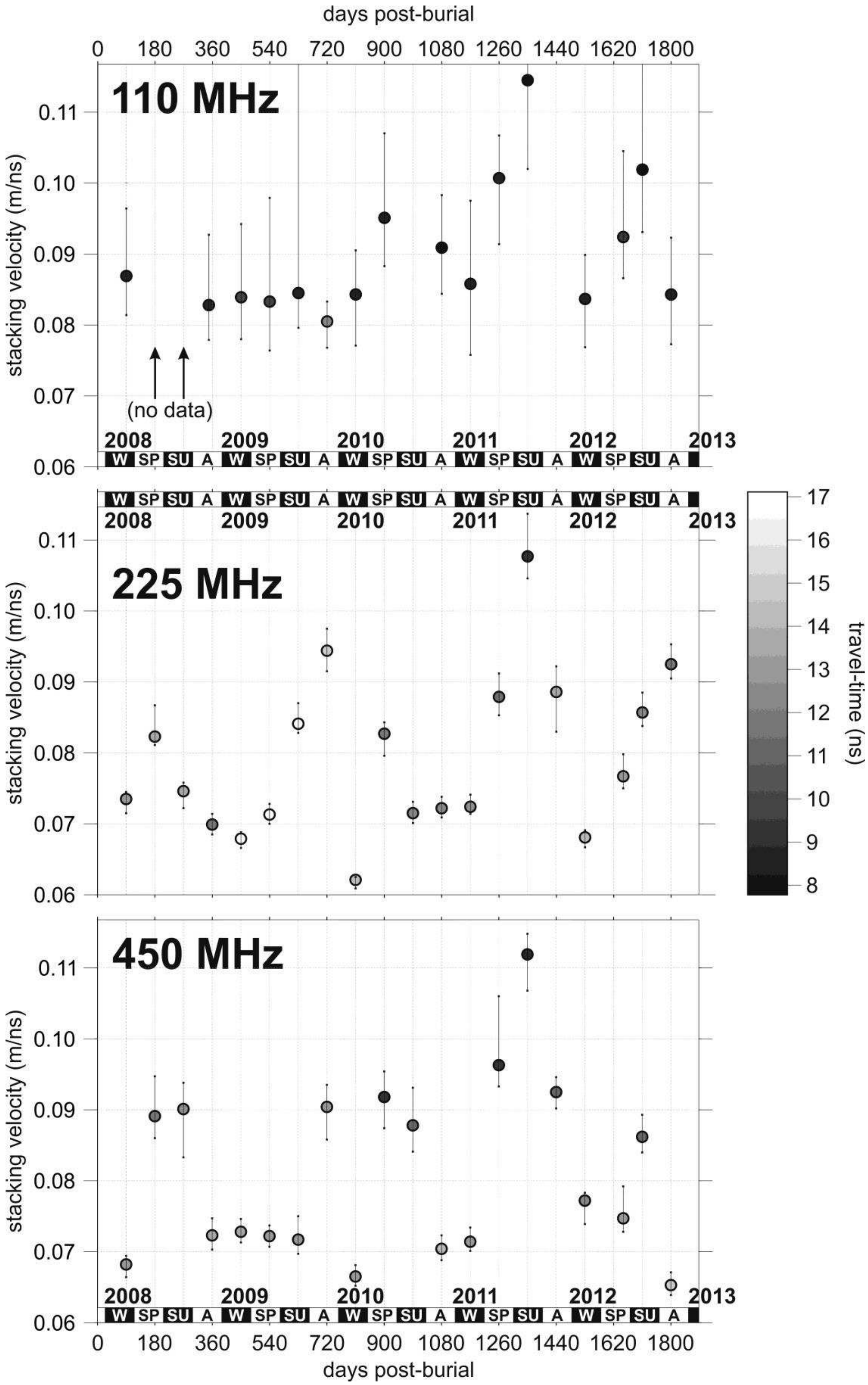

Fig. 5. Time series of stacking velocity (symbols) with velocity resolution (error bars) and travel-time (symbol colour), calculated by semblance analysis of 110 MHz, 225 MHz and 450 MHz diffraction hyperbolae data.

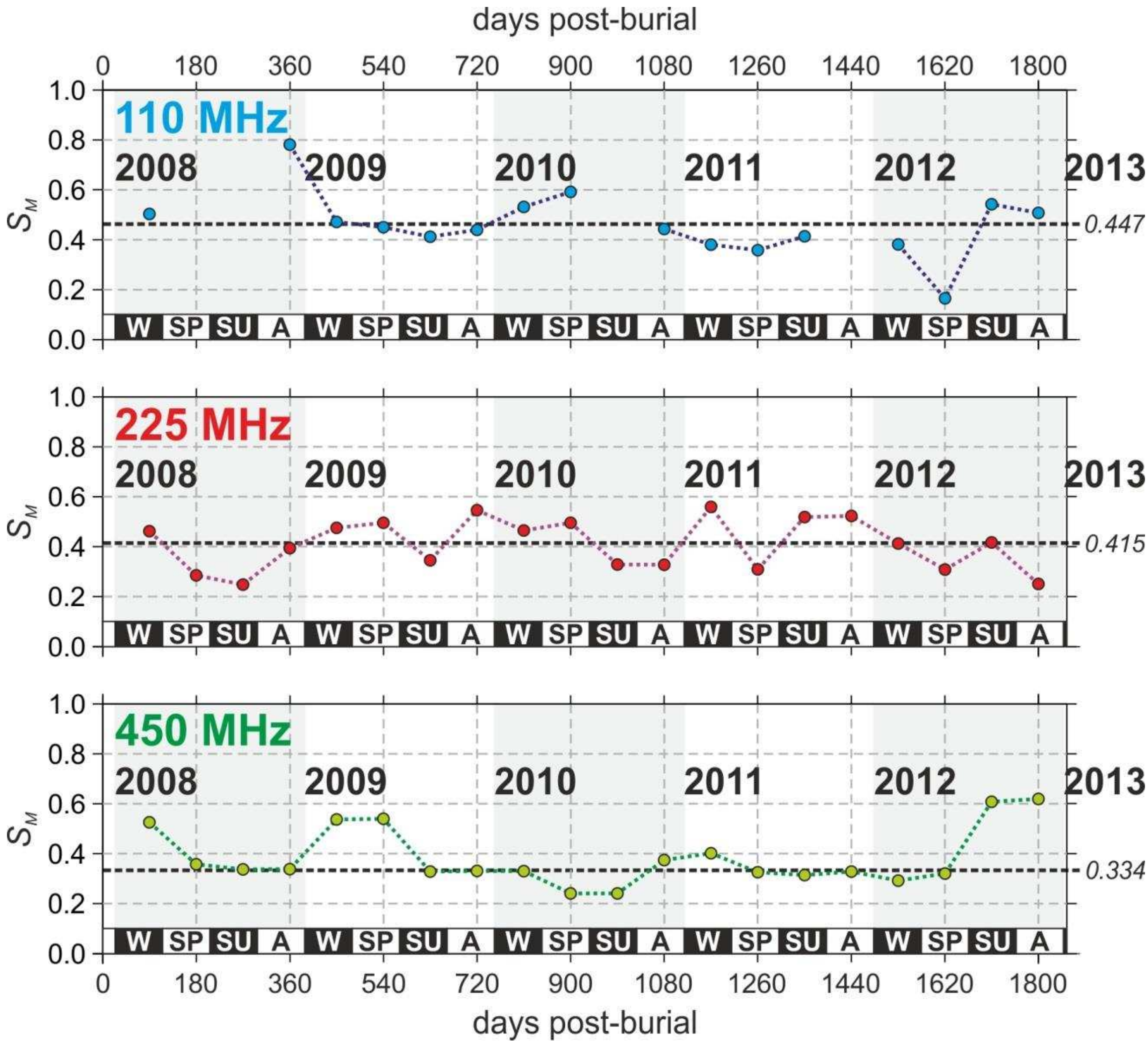

Fig. 6. Time series of semblance magnitude, S_M, expressed by semblance analysis of 110 MHz, 225 MHz and 450 MHz diffraction hyperbolae.

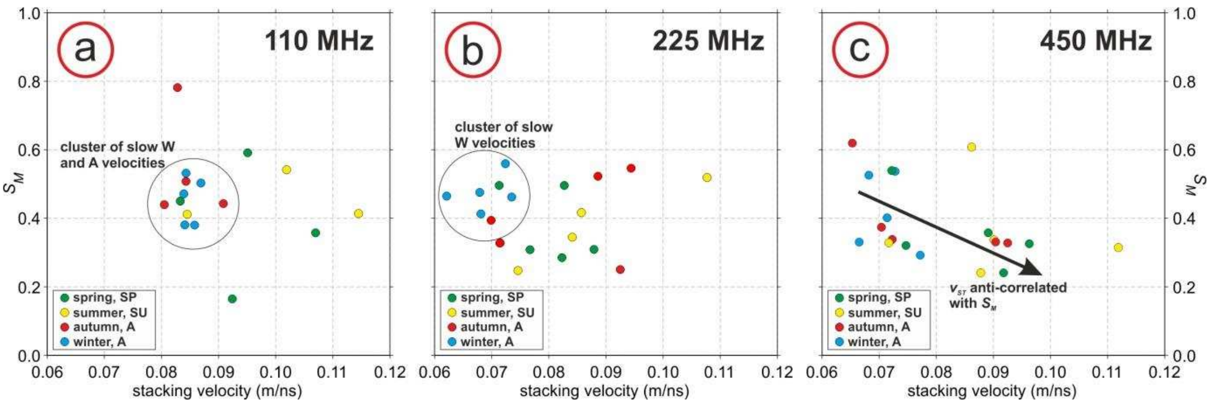

Fig. 7. Crossplots of V_{ST} versus S_M for (a) 110 MHz, (b) 225 MHz and (c) 450 MHz profiles. Symbols are coloured according to season acquired (see legend).

While we cannot exclude velocity and/or reflectivity changes associated with variations in the geometry of the burial over time (see Shibab and Al-Nuaimy, 2005), as the pig cadaver gradually decomposes, combined V_{ST} and $t(x_0)$ quantities consistently estimate the depth of the burial as 0.50 m ± 0.07 m, suggesting that geometric changes were not significant.

5. Discussion

In their study of simulated grave sites, Jervis and Pringle (2014) quantified the resistivity response of wrapped- and naked-pig burials over a five year monitoring period, and cautioned that seasonal variations may make grave-related anomaly(s) undetectable at certain times of the year. Although limited primarily to the study of the wrapped-pig grave, the semblance analyses we have performed show, by contrast, no evidence of a systematic evolution of GPR properties over the course of the survey, and only a small seasonal control on the responses. GPR methods are therefore unlikely to be readily sensitive to changes in the condition of a burial, and are instead more directly influenced by the environmental state (e.g., water content) of the host soil material. This insensitivity likely impedes forensic application of GPR to date a burial. However, by contrast with resistivity methods (Jervis and Pringle, 2014), there was also no time of the year which could be described as obstructive to GPR methods hence a forensic search team could expect similar results from the GPR survey regardless of when the survey was conducted.

The highest semblance magnitudes were typically observed for the 110 MHz data (their mean S_M was 13%, and 20%, higher than those of the 225 MHz and 450 MHz series, respectively), presumably because SNR in the low frequency dataset was higher given the reduced signal attenuation. While antenna frequencies should be chosen on a site and/or target-specific basis, we suggest that semblance analysis offers no practical limitation on the lowest recommendable frequency, an observation made by other researchers (e.g. Schultz and Martin, 2011; Pringle et al. 2012b).

Semblance analysis was lastly a promising means of objectifying the assessment of GPR data profiles, but only where targets (such as wrapped-pig burials) were expressed as diffraction hyperbolae. The method would be unsuitable for assessing data in which targets do not present as prominent diffractions, including the majority of the 2D profiles acquired over the naked pigs (Pringle et al. 2012b). However, in these cases, it may be possible to conduct equivalent semblance analyses but for data acquired as CMP gathers, although these are significantly more time-consuming to collect (see Booth et al. 2010b). A future development of the method would be to incorporate the finite offset of the GPR antennas into the semblance calculation or, alternatively, obtain the zero-offset response from the CO profile by the application of dip moveout (DMO) methods (e.g. see Jakubowicz, 1990). In this way, semblance-derived parameters would be more interpretable in terms of the underlying physical properties of the subsurface and, potentially, the geometry of the burial.

6. Conclusions

This study showed an objective means of assessing GPR diffraction hyperbolae from simulated graves, with semblance-derived quantities of stacking velocity, velocity resolution and semblance magnitude all useful to this end. Data from our wrapped-pig grave were consistently amenable to semblance analysis, featuring strong diffraction hyperbolae. The lowest frequency (110 MHz) acquisition consistently featured the highest signal-to-noise ratio responses, albeit with the lowest resolution.

In contrast to the electrical resistivity surveys detailed in Jervis and Pringle (2014), there was no detectable long-term temporal trend observed with the GPR data over the survey period (although Pringle et al. (2012b) noted a qualitative tendency for hyperbolae to reduce in amplitude as more time since burial elapsed). This gives confidence that GPR could detect a wrapped burial much older than five years in a comparable study setting of a sandy loam, semi-rural, environment. Subtle seasonal variations were observed with increased velocities and lower reflectivity in summer months, but not to the extent that seasonality would preclude imaging and GPR application.

We recommend further development of quantitative GPR analysis of forensic data, and suggest further research on control data, from a range of study settings, to validate the derivation of subsurface properties and determine the long-term sensitivity of semblance analysis to established decomposition trends.

Acknowledgements

Jon Jervis and Jamie Hansen (formerly PhD students at Keele University) are thanked for their assistance with data collection. Access to ReflexW© processing software was part-funded by The Hajar Project. Initial trials of common offset semblance analysis were performed by Emma Smith during her MSc Exploration Geophysics degree at the University of Leeds, using code initially authored by Brian Barrett. Two anonymous reviewers provided a thorough assessment of this manuscript.

Appendix A. Supplementary data

Raw GPR profiles will be made downloadable as Sensors&Software formatted data files, in a WinZip archive. [**NOTE TO EDITOR**/**REVIEWER**: These will be uploaded at a later date, as I couldn't upload them as a single Zip file through the journal website].

References

Amendt, J., Campobasso, C.P., Gaudry, E., Reiter, C., LeBlanc, H.N., Hall, M.J.R. 2007. Best practice in forensic entomology: standards and guidelines, Int. J. Legal Med. 121, 90-104. http://dx.doi.org/10.1007/s00414-006-0086-x

Aquila, I., Ausania, F., Di Nunzio, C., Serra, A.. Boca, S., Capelli, A., et al. 2014. The role of forensic botany in crime scene investigation: case report and review of literature. J. For. Sci. 59, 820-824. http://dx.doi.org/10.1111/1556-4029.12401

Billinger, M.S., 2009. Utilizing ground penetrating radar for the location of a potential human being under concrete. Can. Soc. For. Sci. J. 42, 200-209. http://dx.doi.org/10.1080/00085030.2009.10757607

Booth, A.D., Clark, R., Murray, T., 2011. Influences on the resolution of GPR velocity analysis and a Monte Carlo simulation for establishing velocity precision. Near Surf. Geophys. 9, 399-411. http://dx.doi.org/10.3997/1873-0604.2011019

Booth, A.D., Clark, R., Murray, T., 2010a. Semblance response to a ground-penetrating radar wavelet and resulting errors in velocity analysis. Near Surf. Geophys. 8, 235-246. http://dx.doi.org/10.3997/1873-0604.2010008.

Booth, A.D., Clark, R.A., Hamilton, K., Murray, T. 2010b. Multi-offset GPR methods to image buried foundations of a Medieval town wall, Great Yarmouth, UK. Arch. Prosp. 17, 103-116. http://dx.doi.org/10.1002/arp.377

Buck, S.C., 2003. Searching for graves using geophysical technology: field tests with ground penetrating radar, magnetometry and electrical resistivity. J. For. Sci. 48, 5–11. http://dx.doi.org/10.1520/JFS2002053

Calkin S.F., Allen, R.P., Harriman, M.P., 1995. Buried in the basement – geophysics role in a forensic investigation. Proceedings of the symposium on the application of geophysics to engineering and environmental problems; Denver: Environmental Engineering Geophysical Society, 397–403.

Cheetham, P. 2005. Forensic geophysical survey, in: Hunter, J., Cox, M. (Eds.) Forensic archaeology: advances in theory and practice, Routledge, 62–95. ISBN 0-415-27312-9

Davenport, G.C., 2001. Remote sensing applications in forensic investigations. Hist. Arch. 35, 87–100.

Fiedler, S., Illich, B., Berger, J., Graw, M., 2009. The effectiveness of ground-penetrating radar surveys in the location of unmarked burial sites in modern cemeteries. J. Appl. Geophys. 68, 380-385. http://dx.doi.org/10.1016/j.jappgeo.2009.03.003

Fomel, S. Landa, E., 2014. Structural uncertainty of time-migrated seismic images. J. Appl. Geophys., 101, 27-30. http://dx.doi.org/10.1016/j.jappgeo.2013.11.010.

France, D.L., Griffin, T.J., Swanburg, J.G., Lindemann, J.W., Davenport, G.C., Trammell V., et al. 1992. A multidisciplinary approach to the detection of clandestine graves, J. For. Sci. 37, 1445–1458.

Giannopoulos, A., 2005. Modelling of ground penetrating radar data using GprMax. Const. Build. Mat. 19, 755-762. http://dx.doi.org/10.1016/j.conbuildmat.2005.06.007

Hammon, W.S., McMechan, G.A., Zeng, X., 2000. Forensic GPR: finite-difference simulations of responses from buried human remains. J. Appl. Geophys. 45, 171–186. http://dx.doi.org/10.1016/S0926-9851(00)00027-6

Harrison, M., Donnelly, L.J. 2009. Locating concealed homicide victims: developing the role of geoforensics, in: Ritz, K., Dawson, L., Miller, D. (Eds.), Crim. Env. Soil For., Springer, 197–219. http://dx.doi.org/10.1007/978-1-4020-9204-6_13

Hansen, J.D., Pringle, J.K., Goodwin, J. 2014. GPR and bulk ground resistivity surveys in graveyards: locating unmarked burials in contrasting soil types. For. Sci. Int. 237, e14-e29. http://dx.doi.org/10.1016/j.forsciint.2014.01.009

Jakubowicz, H., 1990. A simple efficient method of dip-moveout correction. Geophysical Prospecting, 38(3), 221-245. http://dx.doi.org/10.1111/j.1365-2478.1990.tb01843.x

Jervis, J.R., Pringle, J.K. 2014. A study on the effect of seasonal climatic factors on the electrical resistivity response of three experimental graves. J Appl. Geophys. 108, 53-60. http://dx.doi.org/10.1016/j.jappgeo.2014.06.008

Jervis, J.R., Pringle, J.K., Tuckwell, G.T. 2009. Time-lapse resistivity surveys over simulated clandestine burials. For. Sci. Int. 192, 7-13. http://dx.doi.org/10.1016/j.forsciint.2009.07.001

Kalacska, M., Bell, L.S., Sanchez-Azofeifa, G.A., Caelli, T. 2009. The application of remote sensing for detecting mass graves: an experimental animal case study from Costa Rica. J. For. Sci. 54, 159-166. http://dx.doi.org/10.1111/j.1556-4029.2008.00938.x

Larson, D.O., Vass, A.A., Wise, M. 2011. Advanced scientific methods and procedures in the forensic investigation of clandestine graves. J. Contemp. Crim. Just. 27, 149–182. http://dx.doi.org/10.1177/1043986211405885

Lasseter, A., Jacobi, K.P., Farley, R., Hensel, L. 2003. Cadaver dog and handler team capabilities in the recovery of buried human remains in the Southeastern United States. J For. Sci. 48, 1–5. http://dx.doi.org/10.1520/JFS2002296

Mellet, J.S., 1992. Location of human remains with ground penetrating radar. In: Hanninen, P., Autio S., (Editors), Proceedings of the Fourth International Conference on Ground Penetrating Radar, June 8-13; Rovaniemi, Geological Survey of Finland Special Paper 16, 359–65.

Nobes, D.C., 2000. The search for ‘‘Yvonne’’: a case example of the delineation of a grave using near-surface geophysical methods. J. For. Sci. 45, 715–721. http://dx.doi.org/10.1520/JFS14756J

Novo, A., Lorenzo, H., Ria, F., Solla, M., 2011. 3D GPR in forensics: finding a clandestine grave in a mountainous environment. For. Sci. Int. 204, 134-138. http://dx.doi.org/10.1016/j.forsciint.2010.05.019

Parker, R., Ruffell, A., Hughes, D., Pringle, J., 2010. Geophysics and the search of freshwater bodies: a review. Sci. & Just. 50, 141-149. http://dx.doi.org/10.1016/j.scijus.2009.09.001

Porsani, J.L., Sauck, W.A. and Abad Jr., O.S., 2006. GPR for mapping fractures and as a guide for the extraction of ornamental granite from a quarry: A case study from southern Brazil. J. Appl. Geophys. 58, 177-187. doi:10.1016/j.jappgeo.2005.05.010

Powell, K. 2004. Detecting human remains using near-surface geophysical instruments, Expl. Geophys. 35, 88-92. http://dx.doi.org/10.1071/EG04088

Pringle, J.K., Ruffell, A., Jervis, J.R., Donnelly, L., McKinley, J., Hansen, J., Morgan, R., Pirrie, D., Harrison, M., 2012a. The use of geoscience methods for terrestrial forensic searches. Earth Sci. Rev. 114, 108-123. http://dx.doi.org/10.1016/j.earscirev.2012.05.006

Pringle, J.K., Jervis, J.R., Hansen, J.D., Jones, G.M., Cassidy, N.J., Cassella, J.P., 2012b. Geophysical monitoring of simulated clandestine graves using electrical and ground-penetrating radar methods: 0-3 years after burial. J. For. Sci. 57, 1467-1486. http://dx.doi.org/10.1111/j.1556-4029.2012.02151.x

Pringle, J.K. and Jervis, J.R.. Electrical resistivity survey to search for a recent clandestine burial of a homicide victim, UK, For. Sci. Int. 202 (2010) e1-e7. http://dx.doi.org/10.1016/j.forsciint.2010.04.023

Pringle, J.K., Jervis, J.R., Cassella, J.P., Cassidy, N.J., 2008. Time-lapse geophysical investigations over a simulated urban clandestine grave. J. For. Sci. 53, 1405-1416. http://dx.doi.org/10.1111/j.1556-4029.2008.00884.x

Ristic, A.V., Petrovacki, D., Govedarica, M., 2009. A new method to simultaneously estimate the radius of a cylindrical object and the wave propagation velocity from GPR data. Comp. Geosci. 35, 1620-1630. http://dx.doi.org/10.1016/j.cageo.2009.01.003

Ruffell, A., McKinley, J. 2014. Forensic geomorphology. Geomorph. 206, 14-22. http://dx.doi.org/10.1016/j.geomorph.2013.12.020

Ruffell, A. 2005a. Burial location using cheap and reliable quantitative probe measurements, For. Sci. Int. 151, 207–211. http://dx.doi.org/10.1016/j.forsciint.2004.12.036

Ruffell, A., 2005b. Searching for the IRA “disappeared”: Ground Penetrating radar investigation of a churchyard burial site. J. For. Sci. 50, 1430-1435. http://dx.doi.org/10.1520/JFS2004156

Schultz, J.J., Martin, M.M.., 2012. Monitoring controlled graves representing common burial scenarios with ground penetrating radar. J. Appl. Geophys. 83, 74-89. http://dx.doi.org/10.1016/j.jappgeo.2012.05.006

Schultz, J.J., Martin, M.M., 2011. Controlled GPR grave research: comparison of reflection profiles between 500 and 250 MHz antennae. For. Sci. Int. 209, 64-69. http://dx.doi.org/10.1016/j.forsciint.2010.12.012

Schultz, J.J., 2008. Sequential monitoring of burials containing small pig cadavers using ground-penetrating radar. J. For. Sci. 53, 279–287. http://dx.doi.org/10.1111/j.1556-4029.2008.00665.x

Schultz, J.J., 2007. Using ground-penetrating radar to locate clandestine graves of homicide victims. Homicide Stud. 11, 1-15. http://dx.doi.org/10.1177/1088767906296234

Schultz, J.J., Collins, M.E., Falsetti, A.B., 2006. Sequential monitoring of burials containing large pig cadavers using ground-penetrating radar. J. For. Sci. 51, 607–616. http://dx.doi.org/10.1111/j.1556-4029.2006.00129.x

Shihab, S., Al-Nuaimy, W., 2005. Radius estimation for cylindrical objects detected by ground penetrating radar. Subsurf. Sens. Tech. App. 6, 1-16. http://dx.doi.org/10.1007/s11220-005-0004-1

Vass, A.A. 2012. Odor mortis. For. Sci. Int. 222, 234-241. http://dx.doi.org/10.1016/j.forsciint.2012.06.006

Vaughan, C., 1986. Ground penetrating radar surveys used in archaeological investigations. Geophys. 51, 595-604. http://dx.doi.org/10.1190/1.1442114

Yilmaz, O., 2001. Seismic data analysis. SEG Investigations in Geophysics Series 10. Society of Exploration Geophysicists, Tulsa OK.